Stability of the mode-locked regime in quantum dot lasers

E. A. Viktorov and Paul Mandel[a)]
Optique Nonlinéaire Théorique, Université Libre de Bruxelles, Campus Plaine CP 231, B-1050 Bruxelles, Belgium

M. Kuntz, G. Fiol, and D. Bimberg
Institut für Festkörperphysik, Technische Universität Berlin, Hardenbergstr. 36, 10623 Berlin, Germany

A. G. Vladimirov and M. Wolfrum
Weierstraß Institute for Applied Analysis and Stochastics, Mohrenstrasse 39, D-10117 Berlin, Germany

(Received 28 September 2007; accepted 18 November 2007; published online 7 December 2007)

We report on experimental and theoretical studies of the stability regime of passive mode-locked quantum dot lasers, which is decisively larger than in quantum well lasers. A small range of Q-switched instability is observed at low gain currents. Transition to Q switching is inhibited due to fast damping of the relaxation oscillations. A double pulse mode-locking regime appears for longer cavities, and exhibits bistability and coupling to the fundamental mode-locking operation.
 [DOI: 10.1063/1.2822808]

Passive and hybrid mode-locked (MLd) quantum dot lasers (QDLs) are efficient sources of short pulses ideal for applications in high speed communication systems.[1,2] The mode-locking (ML) regime of quantum well lasers can exhibit peak power fluctuations induced by a Q-switching instability, which is detrimental for the laser performance. In most experimental situations, QDLs have only a small range of Q switching instability, a consequence of the strong damping of the relaxation oscillations induced by the fast carrier capture from the wetting layer to the dots.

In this letter, we study the stability of the mode-locked regime in QDLs with pulse repetition rates of 20 and 40 GHz. We find that stable ML in QDLs occurs in a comparatively larger range of parameters than in quantum well lasers. We also demonstrate the bifurcation to a state of doubled pulse repetition frequency in the MLd regime in longer cavity devices and characterize its coupling to the fundamental ML regime.

The devices used in this work are two-section QDLs with a total length of 1 mm integrated in a module and an unpackaged 2 mm device (saturable absorber length is always 1/10 of the total length). The active region was grown on a GaAs substrate, containing 15 self-organized InAs QD layers. The facet near the absorber was high refection coated, the front facet was as cleaved. Details of the growth and the processing are the same as described in Ref. 2.

A number of different regimes have been observed experimentally: Q-switching modulated ML, pure ML and, finally, cw lasing. The stability domains of these regimes are displayed in Fig. 1 for the 1 mm QDL module. We measured the radio frequency (rf) spectra of the optical output in the range of 0–50 GHz by means of a 55 GHz bandwidth photodetector and a 50 GHz electrical spectrum analyzer. The side band suppression ratio (SBSR) with respect to the fundamental ML frequency at 40 GHz was extracted for a large set of reverse bias voltages and gain currents and plotted in Fig. 1. The large area of proper ML with a SBSR better than 20 dB, i.e., with weak or absent bands besides the fundamental ML frequency, dominates the figure. The region of Q-switching modulated ML, i.e., the region with strong side bands in the range of a few gigahertz, is small compared to that observed with quantum well lasers.[3] Both regions are separated by a steplike change of the SBSR by more than 30 dB. In our experiments, we did not observe any dependence of the SBSR plot on the scanning direction of the bias parameters. Therefore, within the resolution of the parameter scan, no hysteresis between mode-locked, modulated mode-locked, and the nonlasing state was found.

The 1 mm cavity laser exhibits only fundamental ML which remains stable in a wide range of operation. The pulse doubling appears in the 2 mm, 20 GHz device for large values of the gain current and of the absorber reverse bias, as an abrupt transition from fundamental ML. An autocorrelation trace measured for pulse doubling and the corresponding deconvoluted pulse sequence are shown in Fig. 2. The 50 ps delay window shown for the AC measurement in the inset corresponds to the repetition frequency of 20 GHz of the

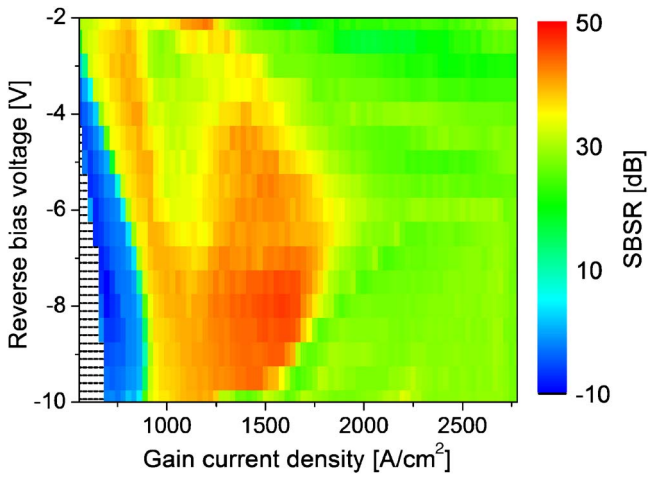

FIG. 1. (Color online) Experimental bifurcation diagram showing the side band suppression ratio (SBSR) relative to the repetition frequency as derived from the rf spectra measurements of the optical output. The blue area denotes strong side bands, corresponding to a strong modulation of ML, whereas the red and green areas denote very weak (>20 dB suppression) or absent side bands, corresponding to pure ML. The patterned area at low currents is the nonlasing domain.

[a)]Electronic mail: pmandel@ulb.ac.be.

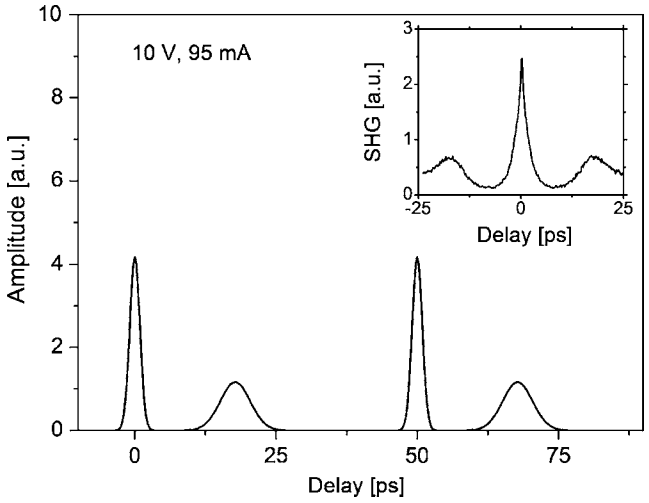

FIG. 2. Autocorrelation trace (inset) and corresponding deconvolution of double pulses at a gain current of 95 mA, absorber reverse bias ≈−10 V, for a ML device of 2 mm length. An asymmetric pulse doubling is observed.

optical pulses. To obtain the pulse sequence, an initial sequence of two Gaussian pulses with variable width, amplitude, and position were numerically convoluted and subsequently fitted to the experimental autocorrelation trace. While traces for currents around 85 mA show pulse doubling with the second pulse appearing in the center between successive fundamental pulses, the traces for 95 mA depict an asymmetric position of the second pulse with respect to the fundamental pulses, i.e., both pulses move closer to each other (Fig. 2). The pulse distance decreases for even higher bias currents. Due to the ambiguous nature of autocorrelation measurements, the position of the smaller second pulse in Fig. 2 could be either leading or trailing, the latter case being shown in the graph. Besides the change in pulse distance, there is a difference in the peak heights and the pulse widths of the two consecutive pulses. The dependence of these characteristics of the double pulse regime on the gain current is shown in Fig. 3. The amplitude of the smaller peak remains nearly constant [Fig. 3(a)] while the amplitude of the larger peak decreases with increasing gain current. The pulse widths show opposite trends: the width of the larger pulse remains almost constant but the width of the smaller pulse significantly decreases [Fig. 3(b)].

In order to explain these instabilities, we use the model of a quantum dot mode-locked laser described in Refs. 4 and 5, which couples the normalized complex amplitude of the electric field $A(t)$, the occupation probabilities in a dot located in the amplifier and in the absorber section $\rho_g(t)$ and $\rho_q(t)$, respectively, and the carrier densities in the wetting layers $N_{g,q}(t)$, scaled to the QD carrier density.

In this model, the time delay T is equal to the cold cavity round trip time. The attenuation factor $\kappa<1$ describes total nonresonant linear intensity losses per cavity round trip. The dimensionless bandwidth of the spectral filtering is γ and the linewidth enhancement factor in the gain (absorber) section is α_g (α_q). The parameters $g_{g,q}$ and τ are, respectively, the differential gains and the relaxation time in the wetting layer and in the dots. All material relaxation times have been assumed to be equal for simplicity. The dimensionless parameters N_{g0} and N_{q0} describe pumping processes in the amplifier and absorber sections. The parameter s is inversely proportional to the saturation intensity. Numerical values are specified in the figure captions.

In the numerical simulations, we use a carrier capture time of $\tau_g=5$ ps for the gain section and $\tau_q=20$ ps for the absorber section. For the escape processes, we use $\tau_g^{\mathrm{esc}}=0.5$ ns in the gain section and $\tau_q^{\mathrm{esc}}=10$ ps in the absorber section. The condition $\tau_q \gg \tau_q^{\mathrm{esc}}$ results from the recent demonstration of the dominant role of the escape processes in the recovery of QD absorber.[6]

A numerical bifurcation diagram is presented in Fig. 4. This diagram, obtained by increasing the gain current N_{g0} at fixed reverse bias $N_{q0}=0.35$, reproduces all main operation regimes that have been observed experimentally: nonlasing state, stable ML, a small region of Q-switch modulated ML, unstable ML regime, ML at higher harmonics, and cw state. No bistability between the ML regime and the nonlasing steady state regime was observed in accordance with the experiments. Typical numerical timetraces illustrating these regimes are shown in Fig. 5.

For $N_{g0}\simeq 0.025$, the fundamental pulsed ML appears and is stable. In Fig. 4, for $N_{g0}\gtrsim 0.04$, the ML pulse is destabilized and a Q-switch modulated ML regime appears [Fig. 5(a)]. As in the experiment, this regime exists in a small region at low gain currents. The modulation frequency is of the order of a few gigahertz corresponding to the relaxation oscillation frequency. The relaxation oscillation frequency is

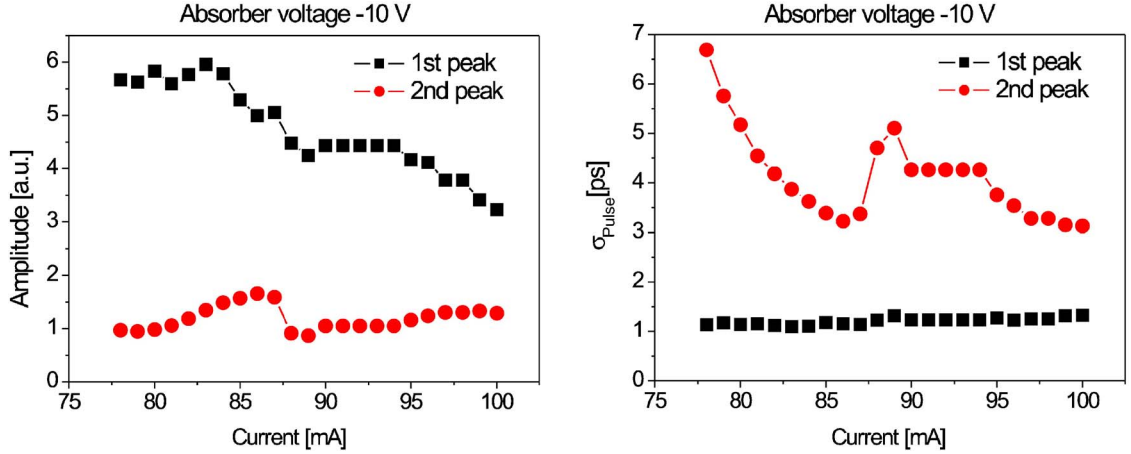

FIG. 3. (Color online) Characteristics of the double pulse regime vs gain current: (a) pulse peak intensity heights and (b) pulsewidth.

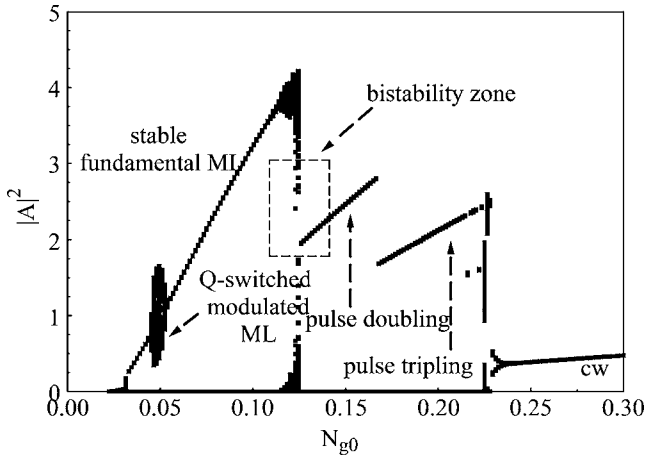

FIG. 4. Numerical bifurcation diagram illustrating transitions between different operation regimes. Parameters are $T=50$ ps, $\kappa=0.34$, $\gamma^{-1}=0.5$ ps, $\tau=1$ ns, $\alpha_g=\alpha_g=2$, $2g_gL_g=3.4$, $2g_qL_q=2.1$, $s=15$, and $N_{q0}=0.35$.

strongly damped in QDLs (Ref. 7) and the damping rate increases with frequency.[8] Stable pulsed ML appears again for $N_{g0}\gtrsim 0.06$ [Fig. 5(b)] and remains stable up to $N_{g0}\simeq 0.10$. Let $G(t)=2g_gL_g[2\rho_g(t)-1]$ and $Q(t)=2g_qL_q[2\rho_q(t)-1]$ be the dimensionless saturable gain and absorption. The round-trip net gain parameter $\mathcal{G}(t)=G(t)-Q(t)+\ln\kappa$ is negative between pulses for $N_{g0}\lesssim 0.09$ and becomes positive only during the short duration of large pulse amplitudes. Therefore, the ML regime in this region is stable with respect to small perturbations of the zero-intensity background.[9]

The observed ML pulse doubling (2 mm cavity) in contrast to only fundamental ML (1 mm cavity) agrees with theoretical results[10] indicating that a decrease of the laser cavity length leads to the suppression of harmonic ML regimes. In this model, a pulse doubling regime appears at $N_{g0}\gtrsim 0.10$, as shown in Fig. 5(c). Numerical simulations reveal the existence of a small range of bistability between the fundamental ML and the pulse doubling regime. In this range, visible in Fig. 4, the fundamental ML pulse has positive net gain at the leading edge (unstable background). The background of the pulse doubling ML is stable. The fundamental ML regime becomes unstable with the appearance of the pulse doubling regime and is weakly amplitude modulated. This instability evolves to chaos at larger gain currents [Fig. 5(d)]. The weak modulation and its evolution to chaos appear only for nonzero α factors. It indicates that the coupling between the fundamental and the higher harmonics depends strongly on the nonlinear phase-amplitude interactions.

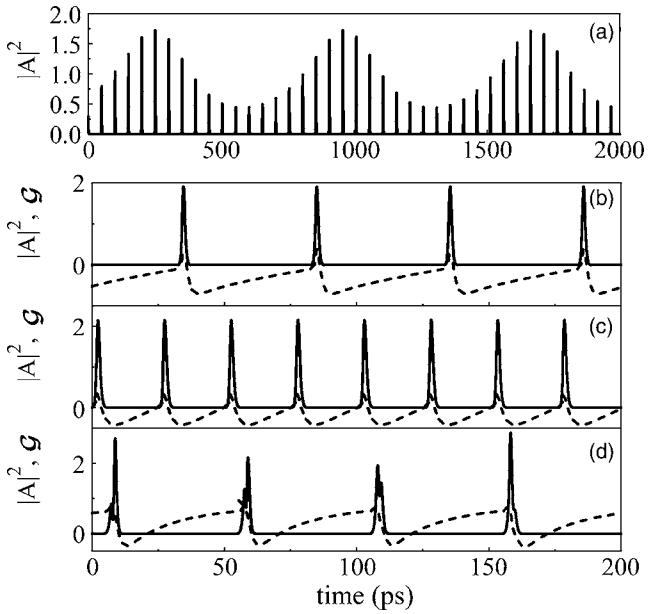

FIG. 5. Time traces in different operating regimes obtained numerically for the laser intensity $|A(t)|^2$ (solid line) and the net gain parameter $G(t)$ (dotted line). (a) Q-switching modulated ML, (b) fundamental ML with pulsewidth ≈ 2 ps, (c) double pulse ML with the pulsewidth ≈ 1.5 ps, and (d) chaotically modulated ML. The regimes (c) and (d) coexist. Parameters are (a) $N_{g0}=0.05$, (b) $N_{g0}=0.07$, (c) and (d) $N_{g0}=0.135$. Other parameters are as for Fig. 4.

Further increase of the gain current leads to a sequence of higher harmonics which eventually ends up in cw operation. Shorter cavities do not lead to significant changes in the bifurcation diagram and for $T=25$ ps, the dynamics remains qualitatively the same as in Fig. 4, but the appearance of the ML at higher harmonics is less likely as explained above. It confirms the better stability of the fundamental ML at shorter cavity as observed experimentally.

In conclusion, we studied instabilities of passive ML in quantum dot lasers. The experiments demonstrate and the theory confirms, that the ML operation in QD lasers has a domain of stability which is significantly larger than that for quantum well lasers. Our model explains the appearance of instabilities either as a Q-switch modulation at low gain currents or in the domain of bistability between the fundamental ML and the double pulse ML regimes observed in devices with 2 mm cavity length.

The authors in Brussels acknowledge support of the Fonds National de la Recherche Scientifique (Belgium). The authors in TUB would like to acknowledge the funding of this work by the SANDiE NoE of the European Commission, Contract No. NMP4-CT-2004-500101, ProFIT MonoPic, and SFB787 of the DFG. The MBE growth of the wafers was done by Innolume GmbH, Dortmund. We would like to thank A. Steffan and A. Umbach from u2t Photonics, Berlin, for the packaging of the MLL module.

[1] D. Bimberg, M. Grundmann, and N. N. Ledentsov, *Quantum Dot Heterostructures* (Wiley, New York, 1999).
[2] D. Bimberg, J. Phys. D **38**, 2055 (2005).
[3] U. Bandelow, M. Radziunas, A. G.Vladimirov, B. Huettl, and B. H. R. Kaiser, Opt. Quantum Electron. **38**, 495 (2006).
[4] A. G. Vladimirov and D. Turaev, Phys. Rev. A **72**, 033808 (2005).
[5] E. A. Viktorov, P. Mandel, A. G. Vladimirov, and U. Bandelow, Appl. Phys. Lett. **88**, 201102 (2006).
[6] D. B. Malins, A. Gomez-Iglesias, S. J. White, W. Sibbett, A. Miller, and E. U. Rafailov, Appl. Phys. Lett. **89**, 171111 (2006).
[7] M. Kuntz, N. N. Ledentsov, D. Bimberg, A. R. Kovsh, V. M. Ustinov, A. E. Zhukov, and Y. M. Shernyakov, Appl. Phys. Lett. **81**, 3846 (2002).
[8] T. Erneux, E. A. Viktorov, and P. Mandel, Phys. Rev. A **76**, 023819 (2007).
[9] G. H. C. New, IEEE J. Quantum Electron. **10**, 115 (1974).
[10] M. Nizette, D. Rachinskii, A. G. Vladimirov, and M. Wolfrum, Physica D **218**, 95 (2006).